The Astrophysical Journal, 678:635–646, 2008 May 10

QUASAR CLUSTERING AT 25 h^{-1} kpc FROM A COMPLETE SAMPLE OF BINARIES[1]

Adam D. Myers,[2] Gordon T. Richards,[3] Robert J. Brunner,[2,4] Donald P. Schneider,[5] Natalie E. Strand,[6] Patrick B. Hall,[7] Jeffrey A. Blomquist,[3] and Donald G. York[8]

Received 2007 September 21; accepted 2008 January 18

ABSTRACT

We present spectroscopy of binary quasar candidates, with component separations of $3'' \leq \Delta\theta < 6''$, selected from Data Release 4 of the Sloan Digital Sky Survey (SDSS DR4) using kernel density estimation (KDE). Of our 27 new quasar pair observations, 10 are binary quasars, which doubles the number of known $g < 21$ binaries with $3'' \leq \Delta\theta < 6''$ separations. Several of our observed binaries are wide-separation lens candidates that merit additional higher resolution spectroscopy, as well as deep imaging to search for lensing galaxies. Our candidates are initially selected by UV excess ($u - g < 1$), but are otherwise selected irrespective of the relative colors of the quasar pair, and we thus use them to suggest optimal color similarity and photometric redshift approaches for targeting binary quasars or projected quasar pairs. We find that a third or more of all binary quasars have quite dissimilar components on the basis of a typical color similarity criterion ($\chi^2_{\rm color} \lesssim 20$). From a sample that is complete on proper scales of 23.7 h^{-1} kpc $< R_{\rm prop} <$ 29.9 h^{-1} kpc, we determine the projected quasar correlation function to be $\bar{W}_p = 24.0^{+16.9}_{-10.8}$, which is 2 σ lower than recent estimates. We argue that our low $\bar{W}_p$ estimates may indicate redshift evolution in the quasar correlation function from $z \sim 1.9$ to $z \sim 1.4$ on scales of $R_{\rm prop} \sim 25\ h^{-1}$ kpc. The size of this evolution broadly tracks quasar clustering on larger scales, consistent with merger-driven models of quasar origin. Spectroscopy of all of our DR4 KDE binary quasar candidates should be sufficient to detect quasar clustering evolution at $R_{\rm prop} \sim 25\ h^{-1}$ kpc for $z < 2.5$ in a single homogeneous sample.

Subject headings: cosmology: observations — large-scale structure of universe — quasars: general — surveys

Online material: color figures

1. INTRODUCTION

Cosmologically, quasars can now be explained as one spectacular stage of an evolutionary process initiated by gas-rich galaxy mergers (see, e.g., Hopkins et al. 2006, 2007). That quasar activity might trace the early stages of merger-driven galaxy evolution makes quasar observations an essential ingredient in constraining galaxy formation scenarios. On the other hand, less luminous active galactic nuclei (AGNs), particularly at low redshift ($z \lesssim 1$), may be better explained by less violent fueling mechanisms (e.g., Hopkins & Hernquist 2006) than the mergers that drive quasars' optical intensity. Given that orientation can complementarily explain many differences within the AGN zoo (e.g., Antonucci 1993; Elvis 2000), new AGN constraints over a broad range of luminosity, particularly across $z \sim 1$, may be key to determining which elements of quasar behavior are mainly structural and which are mainly evolutionary.

If quasars are associated with galaxy mergers, observations of binary quasars with proper separations comparable to the scale of small galaxy groups should offer interesting constraints. Further, there are only a small number of known gravitational lenses with component separations of around $3'' \leq \Delta\theta < 10''$, and there are several plausible arguments as to why most quasar pairs with such separations must be binaries rather than lenses (Bahcall et al. 1986; Phinney & Blandford 1986; Kochanek et al. 1999; Rusin 2002; Oguri 2006; Inada et al. 2008). This makes quasar pairs with separations of around $3'' \lesssim \Delta\theta < 10''$ an ideal target sample with which to study quasar formation in the context of mergers. AGN activity can be excited by tidal forces in galaxy mergers (Barnes & Hernquist 1996; Bahcall et al. 1997), and it has long been argued that this might explain an excess of binary quasars (Djorgovski 1991; Kochanek et al. 1999; Mortlock et al. 1999) and physical triples (Djorgovski et al. 2007). Hopkins et al. (2008) suggest instead that a binary quasar excess simply reflects the increased probability for mergers to occur in regions that are overdense on small scales. If quasars form in mergers, they will thus be naturally more biased at small scales. Hopkins et al. (2008) further argue that orbits for which quasar activity might be excited in both of two merging galaxies are prohibitively rare, even if few such events are needed to explain a binary quasar excess (Kochanek et al. 1999; Myers et al. 2007b, hereafter M07b).

The Sloan Digital Sky Survey (SDSS; York et al. 2000) has renewed interest in binary quasars, and Hennawi et al. (2006, hereafter H06) have used SDSS data to categorically confirm earlier evidence (e.g., Djorgovski 1991; Hewett et al. 1998) that quasar clustering is enhanced on comoving scales of $\lesssim$100 h^{-1} kpc (proper scales of $\lesssim$40 h^{-1} kpc at $z \sim 1.5$). Binary quasars are scarce, with perhaps fewer than 500 in the entire sky to $g \lesssim 21$, redshifts of $z \lesssim 2.5$, and comoving separations of $\lesssim$100 h^{-1} kpc (given the sample size in M07b). Deep, wide imaging, such as that from the SDSS, is thus key to starting to provide new constraints on the cosmological nature of binary quasars. For instance, because of the evolving gas content of the universe, one might expect different redshift evolution in small-scale quasar clustering if it is due to

[1] Some data presented here were obtained at Kitt Peak National Observatory, a division of the National Optical Astronomy Observatory, which is operated by the Association of Universities for Research in Astronomy, Inc., under cooperative agreement with the National Science Foundation.

[2] Department of Astronomy, University of Illinois at Urbana-Champaign, Urbana, IL 61801; admyers@astro.uiuc.edu.

[3] Department of Physics, Drexel University, 3141 Chestnut Street, Philadelphia, PA 19104.

[4] National Center for Supercomputing Applications, Champaign, IL 61820.

[5] Department of Astronomy and Astrophysics, 525 Davey Laboratory, Pennsylvania State University, University Park, PA 16802.

[6] Department of Physics, University of Illinois at Urbana-Champaign, Urbana, IL 61801.

[7] Department of Physics and Astronomy, York University, Toronto, ON M3J 1P3, Canada.

[8] Department of Astronomy and Astrophysics, University of Chicago, Chicago, IL 60637.

a gas-driven effect, such as tidal forces increasing quasar activity, rather than simply being due to the enhanced bias of the dark matter environments in which mergers are likely to occur. Further, some merger-driven models predict stronger small-scale clustering for quasars than for lower luminosity AGNs, due to their different fueling mechanisms (e.g., Hopkins et al. 2008).

Binary quasar samples are typically assembled from pairs that are initially targeted as possible gravitational lenses (e.g., Mortlock et al. 1999; H06). Because of this, the two members of most known binary quasars have similar colors. Although color similarity may be optimal in detecting lenses, scatter in the quasar color-redshift relation (e.g., Richards et al. 2001) dictates that strict color similarity cannot select *all* binary quasars. As binary quasars are useful in testing merger-driven models of quasar activity, it is disconcerting that color similarity cuts might discard particularly informative binaries, such as any that are being excited by tidal forces in merging galaxies. Further, as binary quasars are scarce, relaxing color criteria might help provide enough binaries for us to be able to study their redshift evolution.

We have now performed spectroscopy on a sample drawn from a complete, ultraviolet excess (UVX; $u - g < 1$) set of SDSS Data Release 4 (DR4; Adelman-McCarthy et al. 2006) binary quasar candidates (see Table 1 of M07b). The sample, ∼45% of which has now been identified, is photometrically selected using the kernel density estimation (KDE) technique of Richards et al. (2004). Our aim is to compile an extensive, homogeneous set of binary quasars with proper separations of $\lesssim 40\ h^{-1}$ kpc, mainly in order to study quasar clustering on small scales. Spectroscopy of both objects in most of our binary candidates is not included in the main SDSS quasar survey (e.g., Schneider et al. 2007), because our observations probe a fainter magnitude limit, and because SDSS fibers (in single tiles) cannot be placed closer than 55″. Our approach differs from previous studies of binary quasars. In particular, our main goal is to study binary quasars, not gravitational lenses (unlike the samples compiled in, e.g., Kochanek et al. 1999; Mortlock et al. 1999; H06). Thus, excepting our initial UVX cut, our binaries are the first sample selected regardless of the relative colors of the component quasars. This allows an investigation of whether color similarity can be used to optimally target binary quasars (§ 3).

In § 2, we discuss our initial results in compiling a homogeneous, spectroscopic binary quasar sample from the SDSS, and we report 27 sets of new observations of binary quasar candidates. In § 4 we use a subset of these observations to present the first analysis of quasar clustering on small scales using a *complete* spectroscopic sample of binary quasars. All our binaries are selected from the DR4 KDE candidates of M07b and are therefore a straightforward subset of SDSS DR4, which makes our selection function very simple. We correct all magnitudes for Galactic extinction using the maps of Schlegel et al. (1998) unless otherwise noted. We adopt $\Omega_m = 0.27$ and $\Omega_\Lambda = 0.73$, consistent with the 3 year *WMAP* data (Spergel et al. 2007), and $h \equiv H_0/100$ km s^{-1} Mpc^{-1} $= 0.7$. We denote transverse proper (comoving) scales as $R_{\rm prop}$ (R) and radial proper (comoving) scales as $s_{\rm prop}$ (s), respectively.

2. DATA

2.1. *Observations*

2.1.1. *Candidate Selection*

Our candidate binary quasars are photometric objects in SDSS DR4 that are classified as quasars by the KDE technique (Richards et al. 2004), have $u - g < 1$ and $g < 21$, and are within 3″–6″ of another such object. The SDSS *ugriz* filters are described in Fukugita et al. (1996). As in M07b, we inspect our candidates and discard any that are clearly not quasars (close pairs of KDE candidates are occasionally misclassified H II regions in low-redshift galaxies). We restrict our spectroscopy, as well as our analysis, to quasar pairs with angular separations of $\Delta\theta > 3''$, so that components of a pair appear clearly separated in SDSS imaging (e.g., H06). Although scales that are comparable to small galaxy groups or smaller are most useful in testing merger models of quasar activity, our upper limit of $\Delta\theta < 6''$ is somewhat arbitrary, providing a reasonable number of candidates for a small spectroscopic study. Table 1 of M07b lists our 98 DR4 candidate binaries (and a further 13 candidates with $\Delta\theta < 3''$). At $g < 21$ the KDE technique, coupled with a UVX ($u - g < 1$) cut, selects quasars with 95% efficiency and is over 95% complete for redshifts of $0.2 \lesssim z \lesssim 2.4$ (e.g., Richards et al. 2004; Myers et al. 2006, 2007a). Our survey goal is an efficiently classified, statistical sample of binary quasars that are UVX but are otherwise selected irrespective of the relative colors of the components of the binary. At $z \lesssim 2.5$, our selection should thus only bias our sample against those binaries in which one or both of the component quasars is reddened beyond $u - g = 1$.

2.1.2. *Spectroscopy*

Spectroscopy of our DR4 KDE binary quasar candidates was obtained with the Ritchey-Chrétien Spectrograph on the Mayall 4 m telescope at Kitt Peak National Observatory (KPNO) over five nights (UT 2007 February 22–26). We used a $1.5'' \times 98''$ long slit set at the position angle of the candidate binary, which allowed both components to be simultaneously observed. The KPC-10A grating and WG360 blocking filter yielded a resolution of ∼5 Å and a wavelength coverage of ∼3800–7500 Å. The most useful observations were obtained on February 25 and 26, due to cloud and wind on other nights. Over February 25 and 26, the seeing was $\lesssim 1.5''$, which allowed us to spatially separate even our closest binary candidates (∼3″). The survey goals were a positive identification and redshift for each DR4 KDE binary candidate. This typically required a 15 minute exposure when the *fainter* member of the candidate binary was at $g \sim 19.5$ and three 20 minute exposures (or longer) for objects with $g \sim 21$, although the $\gtrsim$70% illuminated Moon on February 25 and 26 typically prevented our $g \sim 21$ candidates from being spectroscopically identified. Spectra were reduced at the telescope, using IRAF.[9] Exposures ceased once a binary candidate could be identified as (1) containing one star or galaxy or (2) containing two quasars with established redshifts. We estimate redshifts using the rest-frame emission wavelengths listed in Table 2 of Vanden Berk et al. (2001).

Tables 1–4 detail our new observations. Table 1 lists objects for which we obtained an identification for only one member of the candidate binary. Table 2 lists confirmed binary quasars. Following H06, we classify quasar pairs with a line-of-sight velocity difference of $|\Delta v_\parallel| < 2000$ km s^{-1} ($s_{\rm prop} < 9.5\ h^{-1}$ Mpc at $\bar{z} = 1.4$) as a binary. Table 3 lists DR4 KDE binary candidates that are actually "projected" quasar pairs (with components that lie at different redshifts), or pairs in which one object is not a quasar. When both redshifts listed in Table 3 have some uncertainty, a binary quasar interpretation can still be ruled out on the basis of strong lines that are observed in both quasars, but at discrepant wavelengths. Pairs that are harder to definitively identify are listed in Table 4 (see § 2.2.2).

[9] Distributed by the National Optical Astronomy Observatory, which is operated by the Association of Universities for Research in Astronomy, Inc., under cooperative agreement with the National Science Foundation.

TABLE 1
DR4 KDE Candidate Binaries for Which We Have Observed One Member

Name	α (J2000.0)	δ (J2000.0)	g	$z_{\rm phot}$ Range	SDSS z	Our z	$\chi^2_{\rm color}$	$\Delta\theta$
SDSS J093014.81+420038.7	09 30 14.816	+42 00 38.71	19.71	1.15, 1.425, 1.50, 0.93	...	0.544?	36.2	5.50
SDSS J093015.01+420033.6	09 30 15.016	+42 00 33.68	20.03	1.85, 2.025, 2.15, 0.62	...	...	36.2	5.50
SDSS J093521.02+641219.8	09 35 21.020	+64 12 19.89	20.99	1.45, 1.775, 2.10, 0.92	...	1.566	24.2	5.55
SDSS J093521.80+641221.9	09 35 21.807	+64 12 22.00	20.96	0.25, 0.375, 0.45, 0.66	...	...	24.2	5.55
SDSS J095840.74+332216.3	09 58 40.746	+33 22 16.31	19.18	1.35, 1.475, 2.10, 0.84	1.891	1.888	6.4	5.33
SDSS J095840.94+332211.5	09 58 40.945	+33 22 11.59	20.64	1.45, 1.725, 2.10, 0.91	...	...	6.4	5.33
SDSS J103939.31+100253.0	10 39 39.317	+10 02 53.01	18.42	0.10, 0.175, 0.25, 0.56	0.161	0.161	161	3.46
SDSS J103939.53+100254.3	10 39 39.532	+10 02 54.40	19.60	0.65, 1.125, 1.55, 0.92	...	...	161	3.46
SDSS J162847.75+413045.4	16 28 47.752	+41 30 45.45	19.81	1.35, 1.525, 1.70, 0.85	...	...	8.2	4.22
SDSS J162848.06+413043.1	16 28 48.069	+41 30 43.19	20.40	1.95, 2.075, 2.20, 0.63	...	0.831?	8.2	4.22

Notes.—Units of right ascension are hours, minutes, and seconds, and units of declination are degrees, arcminutes, and arcseconds. The photometric redshifts $z_{\rm phot}$ are expressed as follows: lowest extent, peak, highest extent, and the probability of the true redshift lying in this range. The "SDSS z" column shows matches to any spectroscopic object in the SDSS DR6 Catalog Archive Server (mainly, e.g., Schneider et al. 2007). The "Our z" column lists our new spectroscopic confirmations from KPNO data. In the "SDSS z" and "Our z" columns, the object is a quasar at the provided redshift, unless otherwise noted. Redshifts labeled with a question mark are based on a single emission line, which is reasonably assumed to be Mg II. The quantity g is not corrected for Galactic extinction. The angular pair separations are denoted by $\Delta\theta$ (in units of arcseconds), and $\chi^2_{\rm color}$ is each pair's color similarity statistic (eq. [1]).

It became clear during our run that, due to time limitations, an additional uniform restriction would be necessary in order for us to obtain a statistically meaningful spectroscopic sample. On the basis of the pairs that we had already observed, we chose to impose a Galactic extinction limit of $A_g < 0.17$. As we will discuss in § 4, this allowed us to construct a complete, homogeneously selected subsample of DR4 binary quasars. Thus, although our photometric targets had no initial A_g cut, all of the objects that we spectroscopically identified are in regions of SDSS DR4 with values of $A_g < 0.17$. This effectively reduces the solid angle of our survey from all 6670 deg^2 of DR4 to around 5210 deg^2.

TABLE 2
Confirmed Binary Quasars in the DR4 KDE Candidate Sample

Name	α (J2000.0)	δ (J2000.0)	g	$z_{\rm phot}$ Range	SDSS z	Our z	$\chi^2_{\rm color}$	$\Delta\theta$
SDSS J1158+1235A	11 58 22.776	+12 35 18.59	19.90	0.45, 0.525, 0.65, 0.55	...	0.596?	4.0	*3.56
SDSS J1158+1235B	11 58 22.989	+12 35 20.31	20.12	0.40, 0.475, 0.65, 0.63	...	0.596?	4.0	*3.56
SDSS J1320+3056A	13 20 22.545	+30 56 22.87	18.60	1.35, 1.475, 1.65, 0.90	1.597	1.595	32.0	*4.74
SDSS J1320+3056B	13 20 22.643	+30 56 18.29	19.92	1.45, 1.575, 1.80, 0.51	...	1.596	32.0	*4.74
SDSS J1418+2441A	14 18 55.418	+24 41 08.92	19.27	0.45, 0.525, 0.70, 0.96	0.573	0.572	2.8	*4.50
SDSS J1418+2441B	14 18 55.536	+24 41 04.71	20.22	0.40, 0.625, 0.70, 0.86	...	0.573	2.8	*4.50
SDSS J1426+0719A	14 26 04.266	+07 19 25.86	20.82	0.95, 1.175, 1.45, 0.99	...	1.312	3.2	4.27
SDSS J1426+0719B	14 26 04.326	+07 19 30.04	20.12	1.00, 1.225, 1.45, 0.97	...	1.309	3.2	4.27
SDSS J1430+0714A	14 30 02.664	+07 14 15.62	20.27	1.00, 1.225, 1.40, 0.97	...	1.246	25.6	5.41
SDSS J1430+0714B	14 30 02.886	+07 14 11.33	19.50	1.05, 1.375, 1.45, 0.97	1.258	1.261	25.6	5.41
SDSS J1458+5448A	14 58 26.165	+54 48 14.85	20.79	1.50, 1.775, 1.95, 0.75	...	1.913	65.6	5.14
SDSS J1458+5448B	14 58 26.728	+54 48 13.19	20.53	1.65, 1.925, 1.95, 0.47	...	1.912	65.6	5.14
SDSS J1606+2900A	16 06 02.812	+29 00 48.79	18.50	0.50, 0.725, 1.00, 0.65	0.770	0.769?	10.8	*3.45
SDSS J1606+2900B	16 06 03.021	+29 00 50.88	18.42	0.70, 0.875, 1.00, 0.92	...	0.769?	10.8	*3.45
SDSS J1635+2911A	16 35 10.148	+29 11 20.65	18.83	1.45, 1.575, 1.80, 0.84	1.586	1.582	25.6	*4.92
SDSS J1635+2911B	16 35 10.306	+29 11 16.19	20.43	1.40, 1.525, 1.85, 0.79	...	1.590	25.6	*4.92

Notes.—We define a binary quasar by a line-of-sight velocity difference of $|\Delta v_\parallel| < 2000$ km s^{-1} in the rest frame of either component. The pair containing SDSS J143002.66+071415.6 has a velocity difference of $|\Delta v_\parallel| = 2000 \pm 400$ km s^{-1}, which is just inside our definition of a binary. Components are denoted A and B such that the position angle from A to B lies between 0° and 180°. In the final column, a preceding asterisk denotes that our spectroscopy alone is insufficient to rule out a lens interpretation for this pair (see § 2.2.1). SDSS J1320+3056A first appeared with a confirmed redshift ($z = 1.587$) in Veron-Cetty et al. (2004). Units of right ascension are hours, minutes, and seconds, and units of declination are degrees, arcminutes, and arcseconds. The photometric redshifts $z_{\rm phot}$ are expressed as follows: lowest extent, peak, highest extent, and the probability of the true redshift lying in this range. The "SDSS z" column shows matches to any spectroscopic object in the SDSS DR6 Catalog Archive Server (mainly, e.g., Schneider et al. 2007). The "Our z" column lists our new spectroscopic confirmations from KPNO data. In the "SDSS z" and "Our z" columns, the object is a quasar at the provided redshift, unless otherwise noted. Redshifts labeled with a question mark are based on a single emission line, which is reasonably assumed to be Mg II. The quantity g is not corrected for Galactic extinction. The angular pair separations are denoted by $\Delta\theta$ (in units of arcseconds), and $\chi^2_{\rm color}$ is each pair's color similarity statistic (eq. [1]).

TABLE 3

CONFIRMED PROJECTED PAIRS IN THE DR4 KDE CANDIDATE SAMPLE

Name	α (J2000.0)	δ (J2000.0)	g	$z_{\rm phot}$ Range	SDSS z	Our z	$\chi^2_{\rm color}$	$\Delta\theta$
SDSS J083258.34+323003.3	08 32 58.348	+32 30 03.35	19.96	2.75, 2.775, 2.80, 0.88	...	0.397	1220	4.28
SDSS J083258.56+323000.0	08 32 58.567	+32 30 00.08	19.59	0.40, 0.425, 0.50, 0.70	...	Star	1220	4.28
SDSS J084257.37+473342.5	08 42 57.378	+47 33 42.56	19.00	0.50, 0.625, 0.70, 0.51	1.552	1.554	2.0	3.42
SDSS J084257.63+473344.7	08 42 57.638	+47 33 44.74	20.45	0.85, 1.775, 2.10, 0.84	...	1.681	2.0	3.42
SDSS J085914.77+424123.6	08 59 14.771	+42 41 23.67	21.02	0.95, 1.375, 1.65, 0.66	...	1.396	4.9	4.28
SDSS J085915.15+424123.5	08 59 15.159	+42 41 23.58	19.22	0.80, 0.975, 1.40, 0.93	0.898	0.902?	4.9	4.28
SDSS J094309.36+103401.3	09 43 09.363	+10 34 01.31	20.07	0.95, 1.525, 1.70, 0.80	...	1.431	20.6	4.57
SDSS J094309.66+103400.6	09 43 09.670	+10 34 00.65	19.24	1.05, 1.325, 1.40, 0.99	1.238	1.240	20.6	4.57
SDSS J111053.63+605347.9	11 10 53.633	+60 53 47.97	18.94	0.65, 0.775, 0.90, 0.96	...	0.793	32.8	5.91
SDSS J111054.10+605343.1	11 10 54.105	+60 53 43.16	20.86	1.55, 1.775, 2.20, 0.68	...	0.552?	32.8	5.91
SDSS J112556.32+143148.0	11 25 56.321	+14 31 48.10	20.70	0.90, 1.325, 1.60, 0.69	...	NELG	18.4	5.19
SDSS J112556.54+143152.1	11 25 56.549	+14 31 52.10	20.38	1.50, 1.725, 2.15, 0.97	...	1.924	18.4	5.19
SDSS J113637.52+563500.4	11 36 37.526	+56 35 00.48	19.94	1.85, 2.075, 2.15, 0.63	...	1.282	29.9	5.78
SDSS J113638.09+563503.9	11 36 38.090	+56 35 03.90	19.02	0.60, 0.675, 0.90, 0.56	...	2.672	29.9	5.78
SDSS J114503.06+660211.3	11 45 03.063	+66 02 11.35	20.09	1.65, 1.825, 2.00, 0.89	...	1.732	39.3	4.92
SDSS J114503.74+660208.6	11 45 03.741	+66 02 08.67	20.24	0.50, 0.675, 0.85, 0.52	...	2.304	39.3	4.92
SDSS J123122.27+493433.8	12 31 22.276	+49 34 33.86	20.63	0.50, 0.725, 0.90, 0.53	...	0.780?	11.5	3.26
SDSS J123122.37+493430.7	12 31 22.378	+49 34 30.75	19.94	1.55, 1.775, 2.15, 0.95	...	1.811?	11.5	3.26
SDSS J150656.86+505610.5	15 06 56.866	+50 56 10.56	19.22	0.65, 0.775, 1.00, 0.75	...	0.775?	10.7	4.00
SDSS J150657.18+505607.9	15 06 57.183	+50 56 07.92	19.75	2.00, 2.225, 2.40, 0.45	...	2.204	10.7	4.00

NOTES.—SDSS J112556.32+143148.0, the NELG, has a redshift of $z = 0.246$. Subsequent to our observations, SDSS J094309.36+103401.3 appeared in Inada et al. (2008) with $z = 1.433$. The redshift for SDSS J123122.37+493430.7 is based on a single C IV emission line, with weak confirming C III]. Units of right ascension are hours, minutes, and seconds, and units of declination are degrees, arcminutes, and arcseconds. The photometric redshifts $z_{\rm phot}$ are expressed as follows: lowest extent, peak, highest extent, and the probability of the true redshift lying in this range. The "SDSS z" column shows matches to any spectroscopic object in the SDSS DR6 Catalog Archive Server (mainly, e.g., Schneider et al. 2007). The "Our z" column lists our new spectroscopic confirmations from KPNO data. In the "SDSS z" and "Our z" columns, the object is a quasar at the provided redshift, unless otherwise noted. Redshifts labeled with a question mark are based on a single emission line, which is reasonably assumed to be Mg II. The quantity g is not corrected for Galactic extinction. The angular pair separations are denoted by $\Delta\theta$ (in units of arcseconds), and $\chi^2_{\rm color}$ is each pair's color similarity statistic (eq. [1]).

TABLE 4

AMBIGUOUS PAIRS IN THE DR4 KDE BINARY QUASAR CANDIDATE SAMPLE

Name	α (J2000.0)	δ (J2000.0)	g	$z_{\rm phot}$ Range	SDSS z	Our z	$\chi^2_{\rm color}$	$\Delta\theta$
SDSS J093424.11+421135.0	09 34 24.112	+42 11 35.05	21.01	1.45, 1.675, 2.20, 0.90	...	Featureless	42.5	4.80
SDSS J093424.32+421130.8	09 34 24.324	+42 11 30.87	20.30	1.00, 1.125, 1.40, 0.99	...	1.339	42.5	4.80
SDSS J120727.09+140817.1	12 07 27.100	+14 08 17.18	20.39	1.60, 1.775, 2.00, 0.89	...	1.801?	10.7	3.95
SDSS J120727.25+140820.3	12 07 27.259	+14 08 20.38	20.27	1.55, 1.775, 1.95, 0.86	...	1.8??	10.7	3.95
SDSS J1235+6836A	12 35 54.783	+68 36 24.78	19.04	2.75, 2.775, 2.80, 0.55	...	1.529??	207	3.51
SDSS J1235+6836B	12 35 55.270	+68 36 27.07	19.70	0.50, 0.625, 1.10, 0.51	...	1.514	207	3.51
SDSS J1507+2903A	15 07 46.909	+29 03 34.15	20.44	0.80, 0.975, 1.25, 0.77	...	0.875?	14.4	4.35
SDSS J1507+2903B	15 07 47.234	+29 03 33.28	19.97	0.70, 0.775, 0.95, 0.66	...	0.862?	14.4	4.35

NOTES.—Redshifts marked with two question marks are derived from a single emission line. This differs from the single question mark notation, as the redshift is based on similar emission in the other component (rather than simply assuming that the emission is Mg II). The ambiguities, and why we conclude that SDSS J1235+6836 and SDSS J1507+2903 are binaries but the other pairs are not, are discussed in § 2.2.2. Units of right ascension are hours, minutes, and seconds, and units of declination are degrees, arcminutes, and arcseconds. The photometric redshifts $z_{\rm phot}$ are expressed as follows: lowest extent, peak, highest extent, and the probability of the true redshift lying in this range. The "SDSS z" column shows matches to any spectroscopic object in the SDSS DR6 Catalog Archive Server (mainly, e.g., Schneider et al. 2007). The "Our z" column lists our new spectroscopic confirmations from KPNO data. In the "SDSS z" and "Our z" columns, the object is a quasar at the provided redshift, unless otherwise noted. Redshifts labeled with a question mark are based on a single emission line, which is reasonably assumed to be Mg II. The quantity g is not corrected for Galactic extinction. The angular pair separations are denoted by $\Delta\theta$ (in units of arcseconds), and $\chi^2_{\rm color}$ is each pair's color similarity statistic (eq. [1]).

TABLE 5

PREVIOUSLY IDENTIFIED DR4 KDE BINARY QUASAR CANDIDATES WITH $3'' \leq \Delta\theta < 6''$

Name	α (J2000.0)	δ (J2000.0)	g	$z_{\rm phot}$ Range	z	$\chi^2_{\rm color}$	$\Delta\theta$
Projected Pairs							
SDSS J024907.77+003917.1	02 49 07.778	+00 39 17.12	19.36	2.00, 2.175, 2.25, 0.48	2.164	36.7	4.90
SDSS J024907.86+003912.4	02 49 07.866	+00 39 12.40	20.63	0.45, 0.675, 0.85, 0.84	Star	36.7	4.90
SDSS J083649.45+484150.0	08 36 49.456	+48 41 50.08	19.31	0.45, 0.675, 0.80, 0.67	0.657	18.0	4.09
SDSS J083649.55+484154.0	08 36 49.554	+48 41 54.06	18.50	1.50, 1.675, 1.95, 0.94	1.712	18.0	4.09
SDSS J090235.35+563751.8	09 02 35.356	+56 37 51.84	20.95	1.15, 1.275, 1.45, 0.98	1.39	4.5	5.42
SDSS J090235.73+563756.2	09 02 35.731	+56 37 56.29	20.56	1.05, 1.225, 1.45, 0.98	1.34	4.5	5.42
SDSS J095454.73+373419.7	09 54 54.735	+37 34 19.79	19.57	0.95, 1.475, 1.65, 0.90	1.544	37.1	3.14
SDSS J095454.99+373419.9	09 54 54.999	+37 34 19.99	18.91	1.45, 1.575, 1.95, 0.94	1.892	37.1	3.14
SDSS J114718.44+123439.8	11 47 18.448	+12 34 39.84	20.91	1.45, 1.625, 2.00, 0.66	1.583	10.2	4.76
SDSS J114718.66+123436.3	11 47 18.668	+12 34 36.33	19.80	2.15, 2.225, 2.60, 0.54	2.232	10.2	4.76
SDSS J120450.54+442835.8	12 04 50.543	+44 28 35.89	19.04	0.95, 1.125, 1.45, 0.98	1.144	5.6	3.06
SDSS J120450.78+442834.2	12 04 50.784	+44 28 34.25	19.48	1.35, 1.725, 1.95, 0.78	1.814	5.6	3.06
SDSS J124948.12+060709.0	12 49 48.127	+06 07 09.04	20.41	2.20, 2.325, 2.65, 0.89	2.001	23.3	5.04
SDSS J124948.17+060714.0	12 49 48.179	+06 07 14.02	20.38	1.85, 2.075, 2.20, 0.58	2.376	23.3	5.04
SDSS J125530.44+630900.5	12 55 30.445	+63 09 00.51	20.30	1.50, 1.675, 1.90, 0.88	1.753	20.0	3.01
SDSS J125530.82+630902.0	12 55 30.823	+63 09 02.09	20.60	1.10, 1.375, 1.50, 0.98	1.393	20.0	3.01
SDSS J142359.48+545250.8	14 23 59.484	+54 52 50.83	18.63	1.00, 1.175, 1.45, 0.973	1.409[I]	31.2	4.94
SDSS J142400.00+545248.7	14 24 00.006	+54 52 48.79	19.93	1.45, 1.575, 1.90, 0.772	0.610[I]	31.2	4.94
SDSS J162902.59+372430.8	16 29 02.594	+37 24 30.85	19.17	0.80, 0.975, 1.10, 0.93	0.923	25.2	4.35
SDSS J162902.63+372435.1	16 29 02.634	+37 24 35.17	19.35	0.70, 0.925, 1.10, 0.98	0.906	25.2	4.35
SDSS J171334.41+553050.3	17 13 34.414	+55 30 50.36	18.88	1.00, 1.375, 1.45, 0.968	1.276[I]	176	5.83
SDSS J171335.03+553047.9	17 13 35.037	+55 30 47.91	19.11	2.00, 2.175, 2.20, 0.686	Star[I]	176	5.83
SDSS J211157.24+091559.3	21 11 57.248	+09 15 59.33	20.73	0.95, 1.275, 1.40, 0.995	...	172	5.06
SDSS J211157.26+091554.2	21 11 57.269	+09 15 54.28	19.83	1.00, 1.325, 1.35, 0.983	Star[S]	172	5.06
Binary Quasars							
SDSS J0959+5449A	09 59 07.060	+54 49 08.09	20.60	1.90, 2.025, 2.15, 0.59	1.956	18.8	3.94
SDSS J0959+5449B	09 59 07.471	+54 49 06.38	20.07	1.40, 1.575, 2.10, 0.90	1.954	18.8	3.94
SDSS J1259+1241A	12 59 55.464	+12 41 51.06	19.99	1.95, 2.175, 2.30, 0.43	2.180	6.5	3.55
SDSS J1259+1241B	12 59 55.617	+12 41 53.81	20.09	1.90, 2.175, 2.25, 0.52	2.189	6.5	3.55
SDSS J1303+5100A	13 03 26.144	+51 00 51.00	20.54	1.50, 2.075, 2.20, 0.82	1.686	4.3	3.81
SDSS J1303+5100B	13 03 26.177	+51 00 47.21	20.37	1.60, 1.775, 2.00, 0.93	1.684	4.3	3.81
SDSS J1337+6012A	13 37 13.085	+60 12 09.70	20.04	1.30, 1.775, 2.05, 0.66	1.721	0.5	3.12
SDSS J1337+6012B	13 37 13.133	+60 12 06.60	18.59	1.50, 1.625, 1.95, 0.94	1.727	0.5	3.12
SDSS J1432−0106A	14 32 28.949	−01 06 13.55	21.10	1.55, 2.125, 2.25, 0.69	2.082	4.1	5.13
SDSS J1432−0106B	14 32 29.247	−01 06 16.06	17.83	1.90, 2.025, 2.15, 0.96	2.082	4.1	5.13
SDSS J1530+5304A	15 30 38.564	+53 04 04.03	20.56	1.45, 1.575, 1.95, 0.65	1.531	7.2	4.11
SDSS J1530+5304B	15 30 38.824	+53 04 00.65	20.70	1.40, 1.725, 2.15, 0.93	1.533	7.2	4.11
SDSS J1637+2636A	16 37 00.881	+26 36 13.71	20.61	0.45, 0.575, 0.85, 0.46	1.961[D]	2.8	3.90
SDSS J1637+2636B	16 37 00.932	+26 36 09.87	19.36	1.40, 1.525, 1.80, 0.64	1.961[D]	2.8	3.90
SDSS J1723+5904A	17 23 17.307	+59 04 42.79	20.31	1.45, 1.725, 2.25, 0.63	1.597	3.9	3.72
SDSS J1723+5904B	17 23 17.421	+59 04 46.41	18.88	1.55, 1.725, 1.90, 0.94	1.604	3.9	3.72
SDSS J2214+1326A	22 14 26.792	+13 26 52.38	20.64	1.55, 2.025, 2.20, 0.85	1.995	35.0	5.81
SDSS J2214+1326B	22 14 27.032	+13 26 57.01	20.34	1.65, 1.825, 2.05, 0.96	2.002	35.0	5.81

TABLE 5—*Continued*

Name	α (J2000.0)	δ (J2000.0)	g	$z_{\rm phot}$ Range	z	$\chi^2_{\rm color}$	$\Delta\theta$
			Confirmed Lenses				
SDSS J1004+4112A	10 04 34.800	+41 12 39.29	18.64	1.55, 1.725, 2.00, 0.94	1.734[i]	1.9	3.76
SDSS J1004+4112B	10 04 34.917	+41 12 42.81	19.04	1.55, 1.725, 2.15, 0.79	1.734[i]	1.9	3.76
SDSS J1206+4332A	12 06 29.648	+43 32 17.57	18.78	1.65, 1.825, 2.05, 0.96	1.789[o]	46.4	3.04
SDSS J1206+4332B	12 06 29.652	+43 32 20.61	19.38	1.95, 2.175, 2.35, 0.53	1.789[o]	46.4	3.04

NOTES.—Components of a binary are denoted A and B such that the position angle from A to B lies between 0° and 180°. This convention differs from H06, from which we take identifications and redshifts, except for objects labeled with superscripts S (taken from the SDSS), D (discovered by Sramek & Weedman [1978], confirmed as a possible lens by Djorgovski & Spinrad [1984], and likely a binary instead; e.g., Kochanek et al. 1999; Peng et al. 1999; Rusin 2002), i (part of the quad lens from Inada et al. 2003), o (Oguri et al. 2005), and I (Inada et al. 2008). Both of the quasars SDSS J162902.59+372430.8 and SDSS J162902.63+372435.1 first appear in Mason et al. (2000). SDSS J1004+4112A was discovered by Cao et al. (1999), and SDSS J1432−0106B by Hewett et al. (1991). We note that we mistakenly listed SDSS J095454.73+373419.7 as lying at $z = 1.554$ in M07b. Units of right ascension are hours, minutes, and seconds, and units of declination are degrees, arcminutes, and arcseconds. The photometric redshifts $z_{\rm phot}$ are expressed as follows: lowest extent, peak, highest extent, and the probability of the true redshift lying in this range. The quantity g is not corrected for Galactic extinction. The angular pair separations are denoted by $\Delta\theta$ (in units of arcseconds), and $\chi^2_{\rm color}$ is each pair's color similarity statistic (eq. [1]).

In all, we spectroscopically identified 49 objects, of which 44 are both members of 22 candidate quasar pairs and 5 are objects from pairs for which we identified only one member. Of the 49 identified objects, 46 are quasars, which confirms that the KDE technique is ∼95% efficient for $A_g \lesssim 0.17$, as was argued (for $A_g \lesssim 0.21$) in Myers et al. (2007a). Of the 22 candidate quasar pairs for which we identified both components, 3 are quasar-nonquasar pairs, 9 are projected quasar pairs (i.e., at disjoint redshifts), and 10 are binary quasars. Several of the 10 binary quasars could, in fact, be lenses (see § 2.2.1). In Table 5 we list previously known quasar pairs (mainly from H06, but see the notes to Table 5 for full details) that also meet the criteria to be included in our DR4 KDE binary candidate sample. Previously known candidates include 12 nonbinaries, 9 binaries, and 2 lenses. Approximately half of the 98 ($3'' \leq \Delta\theta < 6''$) DR4 KDE candidates have now been spectroscopically identified (see Table 6). With the caveat that bright objects may have been observed first, ∼42% of the candidate pairs are binary quasars, and only ∼16% of the pairs contain a nonquasar.

2.2. *Interesting Spectroscopic Pairs*

2.2.1. *Potential Lenses*

Five pairs in Table 2 have sufficiently similar spectra, at our ∼5 Å resolution, that they might be lensed quasars rather than binaries. As lenses with image separations in the range $3'' \leq \Delta\theta < 6''$ are rare (e.g., Inada et al. 2008), particularly for $z \lesssim 2$, we interpret these objects as binaries (see also Kochanek et al. 1999), although they certainly merit higher resolution spectroscopy and, in those cases that remain ambiguous, deep imaging to rule out a lensing galaxy. A lensing interpretation is especially unlikely for the three possible lenses used in our clustering analysis (§ 4), which have ∼5″ separations and, in two cases, dissimilar colors. In Figure 1 we display the spectra of our most likely lens candidates. SDSS J1158+1235A and B, in particular, have almost identical spectra at our resolution.

TABLE 6
BREAKDOWN OF DR4 KDE QUASAR PAIRS WITH $3'' \leq \Delta\theta < 6''$

Category	Number of Confirmed Pairs
Total binary quasar candidates	98
Total now identified	45
Likely binary quasars	19
Quasar pairs separated in redshift	18
Pairs containing ≥1 nonquasars	6
Pairs that are confirmed lenses	2

NOTE.—It is possible that a few more objects listed here as "likely binary quasars" may turn out to be lensed quasars when scrutinized at higher resolution.

2.2.2. *Notes on Ambiguous Binaries*

Table 4 lists four candidates that we could not definitively identify. We conclude that two of these objects are binaries, for

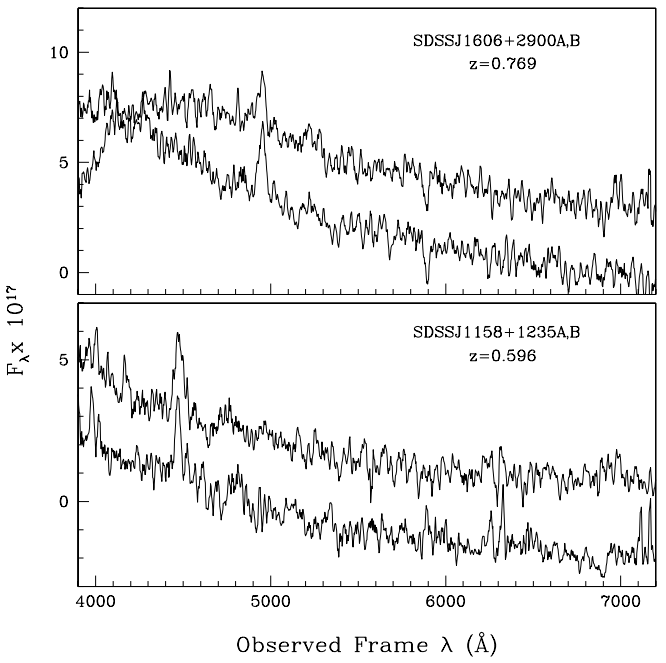

FIG. 1.—Two of the five quasar pairs in our DR4 KDE sample that require higher resolution spectroscopy to determine whether they are binary quasars or a lensed quasar. These spectra were taken with the Ritchey-Chrétien Spectrograph on the Mayall 4 m at KPNO at a resolution of ∼5 Å and have been smoothed with a 5 pixel boxcar. SDSS J1158+1235A,B and SDSS J1606+2900A, B are our two most likely lens candidates, on the basis of their similar colors and component separations of $\Delta\theta < 4''$. In both panels, component A is shown as the upper spectrum and component B has been offset, which can cause component B to have a flux density below zero. In each case, both components are, in reality, at nearly identical flux levels. [*See the electronic edition of the Journal for a color version of this figure*.]

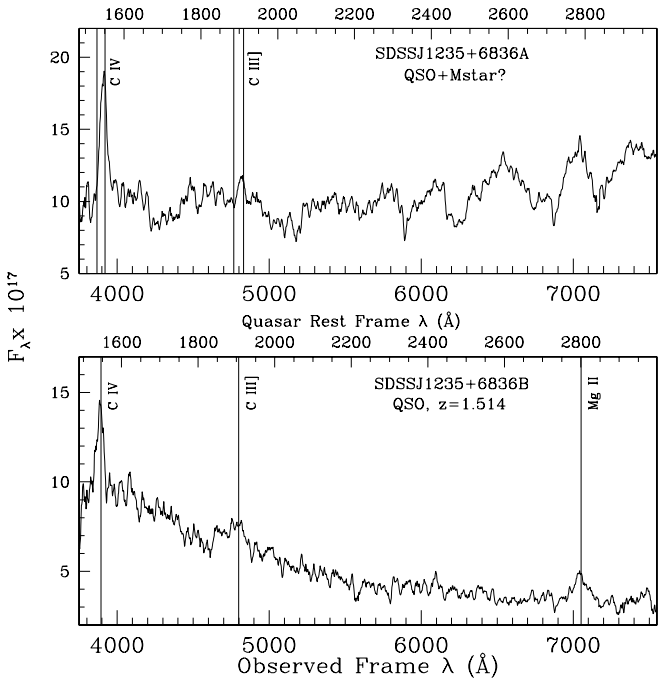

FIG. 2.—Spectra of SDSS J1235+6836A,B, taken with the Ritchey-Chrétien Spectrograph on the Mayall 4 m at KPNO at a resolution of ~5 Å and smoothed with a 5 pixel boxcar. In the bottom panel, the vertical lines mark common quasar emission lines. For component A, in the top panel, emission lines are marked at the systemic redshift of *component B* offset by ±2000 km s^{-1}, a typical window for a binary quasar (e.g., H06). The systemic redshift of component A in Table 4 is derived under the assumption that the emission line near 3900 Å is C IV and is close to the red side of these windows ($z = 1.529$). At red wavelengths, component A resembles an M star. [*See the electronic edition of the Journal for a color version of this figure.*]

the following reasons, where all wavelengths are quoted in the observed frame.

SDSS J093424.32+421130.8 and SDSS J093424.11+421135.0 consist of a quasar at $z = 1.339$ and a featureless spectrum (after 4200 s of exposure). SDSS J093424.11+421135.0 is faint (with an observed $g = 21.01$) and has no obvious emission near 4460 or 6550 Å, which are the principal emission lines used to identify SDSS J093424.32+421130.8. We therefore conservatively conclude that this is not a binary quasar.

SDSS J120727.09+140817.1 and SDSS J120727.25+140820.3 both have ambiguous redshifts. The fainter object (with an observed $g = 20.39$) has broad emission at 4320 Å and near 7840 Å, at the red edge of our coverage. The brighter object ($g = 20.27$) also has possible, low signal-to-noise ratio emission near 4340 Å. We discount this as a matching line, however, as emission in the fainter object is far stronger, and the objects were, obviously, observed under similar conditions. We tentatively conclude that this pair is not a binary quasar.

SDSS J1235+6836A and B (see Fig. 2) are an interesting pair with highly dissimilar colors. SDSS J1235+6836B is apparently a quasar with significant broad emission near 3895 and 7050 Å and weaker emission near 4790 Å. SDSS J1235+6836A is most likely a quasar, with probable broad emission near 3910 Å and possible emission near 4820 Å, lying behind a classic M star observed at the red end of the spectrum. This object may look less like a quasar–M star superposition with time. As a simple quantification of this timescale, there are 15,798 spectral late-type stars in the DR4 Catalog Archive Server that have proper-motion matches in the "USNO" table. The mean proper motion of these objects is 0.0348″ yr^{-1}, which suggests that it will take several decades for the M star to move away from the background quasar.

SDSS J1507+2903A and B have strong emission near 5250 and 5215 Å, respectively. Neither spectrum has additional features over 3800–7500 Å, and so we assume that the emission is Mg II, which places both quasars at $z \sim 0.87$. The ambiguity for this pair is that their redshifts imply that $|\Delta v_{\parallel}| = 2100$ km s^{-1}. Since a shift of $\delta z < 0.0005$, which is far smaller than our typical precision, can bring these quasars to within $|\Delta v_{\parallel}| < 2000$ km s^{-1}, we identify this pair as a binary.

3. COLOR SELECTION OF BINARY QUASARS

To study the relative color selection of binary quasars, we use the χ^2 color similarity statistic introduced by H06,

$$\chi^2_{\rm color}(A) = \sum_{ugriz} \frac{\left(f_2^i - A f_1^i\right)^2}{\left(\sigma_2^i\right)^2 + A^2\left(\sigma_1^i\right)^2}, \quad (1)$$

where the subscripts 1 and 2 represent the components of a pair. The superscript i refers to flux (f) in the five SDSS bands (*ugriz*). For asinh magnitudes (m),

$$f^i = 2F_0 b^i \sinh\left(-m^i/P - \ln b^i\right),$$
$$\sigma_f^i = \left(\sigma_m^i/P\right)\sqrt{(2F_0 b^i)^2 + (f^i)^2}, \quad (2)$$

where $P = 2.5/\ln 10$ (Pogson 1856), $F_0 = 3630.78$ Jy, and $b^{(u,g,r,i,z)} = (1.4, 0.9, 1.2, 1.8, 7.4) \times 10^{-10}$ (Lupton et al. 1999; Stoughton et al. 2002). A quasar pair with more similar colors has a lower value of $\chi^2_{\rm color}$. Iterative equations for calculating A in equation (1) can be ill-conditioned for $\chi^2_{\rm color} \gtrsim 30$, so throughout this work, we numerically determine A by bisection.

Binary quasars are often rejects from gravitational lens searches, and as such, the components of known binaries typically have very similar colors (e.g., SDSS J1637+2636A,B with $\chi^2_{\rm color} = 2.8$: see Table 5; Sramek & Weedman 1978; Djorgovski & Spinrad 1984). Schemes designed to optimize binary quasar searches by selecting pairs with similar colors will therefore naturally reselect known binary quasars. Our DR4 KDE pairs are selected irrespective of the *relative* colors of the components of the pair and should thus be useful in determining color similarity cuts to optimize binary quasar selection. However, some of the quasar pairs in Table 5 were selected by H06 to have $\chi^2_{\rm color} < 20$; as we avoided reobserving these pairs, our data in Tables 2–4 may be biased to $\chi^2_{\rm color} > 20$.

In the top left panel of Figure 3, we demonstrate that the $\chi^2_{\rm color}$ values of the DR4 KDE binary candidates identified to date fairly represent the full sample. We compare the cumulative fraction of the 45 identified candidates (i.e., Table 6) to the remaining 53 ($3'' < \Delta\theta < 6''$) candidates, as a function of $\chi^2_{\rm color}$. A two-sample Kolmogorov-Smirnov (K-S) test cannot distinguish the distributions, which suggests that the relative colors of the observed candidates fairly represent those of all candidates. The top right panel of Figure 3 compares the $\chi^2_{\rm color}$ cumulative probability for the 21 confirmed binary quasars (or lenses) and the 24 confirmed nonbinaries (projected quasar pairs, star-quasar pairs, or narrow emission line galaxy [NELG]-quasar pairs). The K-S test probability that these two distributions are drawn from the same underlying $\chi^2_{\rm color}$ distribution is ~10%, which suggests that $\chi^2_{\rm color}$ can indeed discriminate binary quasars from nonbinaries.

As our candidates are selected without a $\chi^2_{\rm color}$ cut, we can ask what $\chi^2_{\rm color}$ limit optimizes completeness (number of binaries out of 21 total binaries) and efficiency (number of binaries out of

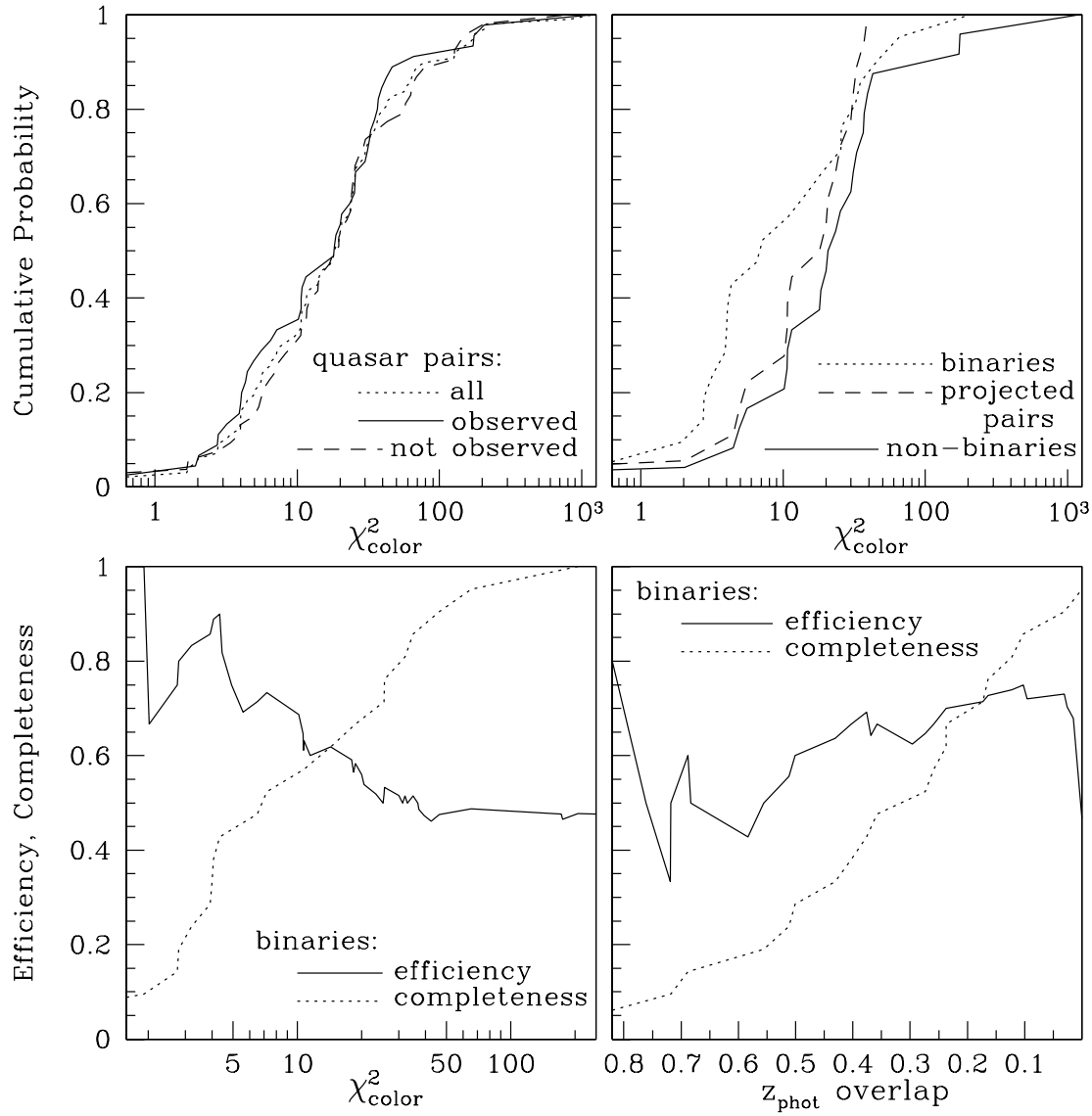

FIG. 3.— *Top left*: Cumulative probability distribution of the χ^2_{color} color similarity statistic (eq. [1]) for the 45 spectroscopically observed DR4 KDE candidate binary quasars, for the 53 that are not yet observed, and for all 98 candidate pairs. *Top right*: Similar to the top left panel, but for the 21 (out of 45) observed candidates that are binary quasars (or lenses), for the 24 (out of 45) candidates that are not binaries, and for the 18 (out of 45) quasar pairs at disjoint redshifts. *Bottom left*: Selection completeness and efficiency effects of imposing a χ^2_{color} limit on the 45 observed DR4 KDE candidate binaries. Efficiency is (number of binaries $< \chi^2_{color}$)/(total candidates $< \chi^2_{color}$); completeness is (number of binaries or lenses $< \chi^2_{color}$)/21. *Bottom right*: Similar to the bottom left panel, but using the fractional overlap of the photometric redshift solutions for the candidate components (z_{phot}) as the determinant of binary selection. Note that a greater overlap in photometric redshift implies a greater color similarity. [*See the electronic edition of the Journal for a color version of this figure*.]

45 observed candidates). To sample $\gtrsim$50% ($\gtrsim$66%) of binary quasars requires a cut of $\chi^2_{color} \lesssim 10$ ($\chi^2_{color} \lesssim 20$), which is efficient at 70% (55%), whereas a cut of $\chi^2_{color} \lesssim 70$–100 contains 95% of all binaries (only missing the "ambiguous" SDSS J1235+6836A,B) and remains 50% efficient. A $\chi^2_{color} < 70$ cut rejects all but one quasar-star pair while retaining all quasar-quasar projections. We also note that although $\chi^2_{color} < 20$ is the "standard" criterion chosen by H06, the additional strategy adopted by H06 of also observing quasars close to a known quasar helped to relax this criterion for their study. For instance, all but one of our $\chi^2_{color} > 20$ binaries in Table 2 contain a known SDSS quasar.

As there is reasonable scatter in the quasar color-redshift relation (e.g., Richards et al. 2001), full photometric redshift (hereafter photo-z) information should better select binary quasars. To test this, we consider the primary color-redshift relation ("CZR") photo-z solution (Weinstein et al. 2004; see "z_{phot} range" in Tables 1–5) for each quasar in our sample. We determine the overlap fraction of the primary photo-z solutions of the two quasars in a pair, multiplying by the probability that the quasar occupies that primary peak. We refer to this quantity as the "z_{phot} overlap" in Figure 3. If the extents of the primary peak (the "z_{phot} range") for each photometric redshift are denoted z_{min} and z_{max}, if the probability of the quasar occupying the primary peak is z_{prob}, and if $A(z)$ is a step function that is 1 for $z_{min} \leq z < z_{max}$ and 0 for all other redshifts, then we calculate the overlap fraction for each member of a quasar pair as

$$O_{1,2} = z^1_{prob} \frac{\int A^1(z) A^2(z)\, dz}{\int A^1(z)\, dz}, \quad (3)$$

and the quantity expressed as the z_{phot} overlap in Figure 3 is the product $O_{1,2}O_{2,1}$. This quantity is clearly only a first-order estimate,

TABLE 7
Complete, Statistical Clustering Subsample

Name	$\Delta\theta$ (arcsec)	$\chi^2_{\rm color}$	$R_{\rm prop}$	R	z_A	z_B	$\lvert\Delta v_\parallel\rvert$	Table
SDSS J0959+5449	3.94	18.8	23.8	70.2	1.956	1.954	200	5
SDSS J1320+3056	*4.74	32.0	28.8	74.7	1.595	1.597	200	2
SDSS J1418+2441	*4.50	2.8	20.9	32.8	0.572	0.573	100	2
SDSS J1426+0719	4.27	3.2	25.6	59.5	1.312	1.309	400	2
SDSS J1458+5448	5.14	65.6	31.1	90.2	1.913	1.912	0	2
SDSS J1507+2903	4.35	14.4	23.8	44.3	0.875?	0.862?	2100	4
SDSS J1530+5304	4.11	7.2	24.9	63.1	1.531	1.533	200	5
SDSS J1635+2911	*4.92	25.6	29.9	77.3	1.582	1.590	900	2

Notes.—The DR4 KDE binary quasar candidate sample is now spectroscopically complete for component separations of $3.9'' < \Delta\theta < 5.2''$ for $g < 20.85$ in regions with Galactic absorptions of $A_g < 0.17$. Twenty pairs meet these criteria, and eight of them are (the listed) binary quasars. A preceding asterisk denotes a possible lens (see note in Table 2). The quantity $R_{\rm prop}$ (R) is the transverse proper (comoving) separation (in units of h^{-1} kpc). The quantity $\lvert\Delta v_\parallel\rvert$ is the line-of-sight velocity difference (in units of km s^{-1}). The final column denotes the table in this paper in which we first listed these binaries. The five listed binaries with transverse separations of $23.7 \leq R_{\rm prop} \leq 29.9$ represent a spatially complete subsample for redshifts of $1.03 < z < 2.10$.

as photometric redshift solutions have probabilities outside of their primary peak and are typically more peaked than a step function. Nevertheless, this first-order estimate is sufficient to demonstrate that quasar photometric redshifts can distinguish binary quasars from projected pairs.

The completeness and efficiency of a binary quasar sample obtained by considering the $z_{\rm phot}$ overlap are plotted in the bottom right panel of Figure 3. Confirmed nonbinaries typically have no $z_{\rm phot}$ overlap. A probability cut at >3% overlap will return 90% of binaries and is 73% efficient. The two binaries that are missed are the "ambiguous" SDSS J1235+6836A,B and SDSS J1637+2636A,B, the "A" component of which has a poorly behaved photo-z solution. If one additionally observed all candidates that contained a quasar with a poor photo-z (characterized by a probability of $z_{\rm prob} < 0.5$), 95% of binary quasars would be observed at 69% efficiency. Of course, although cutting on the $z_{\rm phot}$ overlap is a more efficient mechanism for selecting binaries, it does so at the expense of projected quasar pairs. A cut at <3% overlap could therefore be used to discard binary quasars in favor of projected pairs. Projected pairs are, of course, useful for a range of science purposes, such as studying the properties of quasar absorbers near quasars (e.g., Hennawi & Prochaska 2007). Nevertheless, we have demonstrated that quasar photometric redshifts would be sufficient to efficiently target binary quasars (or, alternatively, projected pairs) without prior spectroscopic identification.

In conclusion, if a survey's goal is to select both binary quasars and projected quasar pairs, a cut of $\chi^2_{\rm color} \lesssim 70$ can return 97% of binaries, lenses, and projected pairs (multiplied by, e.g., the 95% completeness of the KDE technique itself) at 93% efficiency. This is hardly surprising, and it further confirms the high efficiency of the KDE technique. Around 50% (66%) of binary quasars have colors as dissimilar as $\chi^2_{\rm color} > 10$ ($\chi^2_{\rm color} > 20$). If a survey's goal is to observe only binary quasars, then a cut of >0.03 in the overlap of the two quasars' photo-z values can achieve this goal. Interestingly, two ($\sim$10%) of the DR4 KDE binary quasars have more dissimilar colors than any of the quasar-quasar projections, which hints that physical interactions may affect the colors of a few binary quasars. Note that one lens (SDSS J1507+2903, listed in Table 5) also has more dissimilar colors than do any of the quasar-quasar projections, but this could be readily explained by differential reddening by the lensing galaxy (see, e.g., Oguri et al. 2006). We stress that all of the analysis in this section applies only to quasars that have been preselected using an efficient photometric classification technique such as the KDE algorithm.

4. PROJECTED QUASAR CLUSTERING AT 25 h^{-1} kpc

With our new observations (Tables 2 and 4), we have now identified all the DR4 KDE binary quasar candidates with $A_g < 0.17$, $g < 20.85$, and $3.9'' < \Delta\theta < 5.2''$. In Table 7 we compile the binaries that meet these criteria. One of the pairs (SDSS J1507+2903) in Table 7 has $\lvert\Delta v_\parallel\rvert \sim 2100$ km s^{-1}, but we reasonably include this pair as having $\lvert\Delta v_\parallel\rvert \lesssim 2000$ km s^{-1} in our analysis. Instead, rejecting SDSS J1507+2903 would lower our estimates of $\bar{W}_p$ (see eq. [4]) by $\sim$10%. The three possible lenses in Table 7 have wide separations ($\Delta\theta \geq 4.5''$), which makes them likely binaries.

We study quasar clustering using the DD/DR estimator (e.g., Shanks et al. 1983) for quasar-quasar (QQ) pair counts compared to expected quasar-random (QR) pair counts:

$$\bar{W}_p = \frac{QQ}{\langle QR\rangle} - 1. \quad (4)$$

Higher order corrections (e.g., Landy & Szalay 1993) reduce to equation (4) for the small scales and large volumes that we consider. We use small-number Poisson errors from Gehrels (1986). Poisson errors are valid on small scales where pair counts are independent (e.g., Croom & Shanks 1996; Myers et al. 2006).

As our clustering sample is a subset of all SDSS DR4 photometric objects, our selection function is very simple. We calculate $\langle QR\rangle$ in equation (4) by constructing a catalog of random points with the same angular coverage as the SDSS DR4, correcting the SDSS data for mask holes, as in Myers et al. (2006, 2007a). We further limit our random catalog to areas of the sky with Galactic absorptions of $A_g < 0.17$. We assign random points a redshift according to a fit to the normalized redshift distribution of ($A_g < 0.17$, $g < 20.85$) quasars in the DR1 catalog (Schneider et al. 2003), from which the DR4 KDE quasar classification is trained. Figure 7 of Myers et al. (2006) is similar to this redshift distribution, and Myers et al. (2006) argue that including additional quasars that overlap the KDE color space minimally impacts this $N(z)$ distribution. To represent our fit, we use a modified Gaussian,

$$dN = \beta \exp\frac{-|z-\bar{z}|^n}{n\sigma_i^n}\, dz, \quad (5)$$

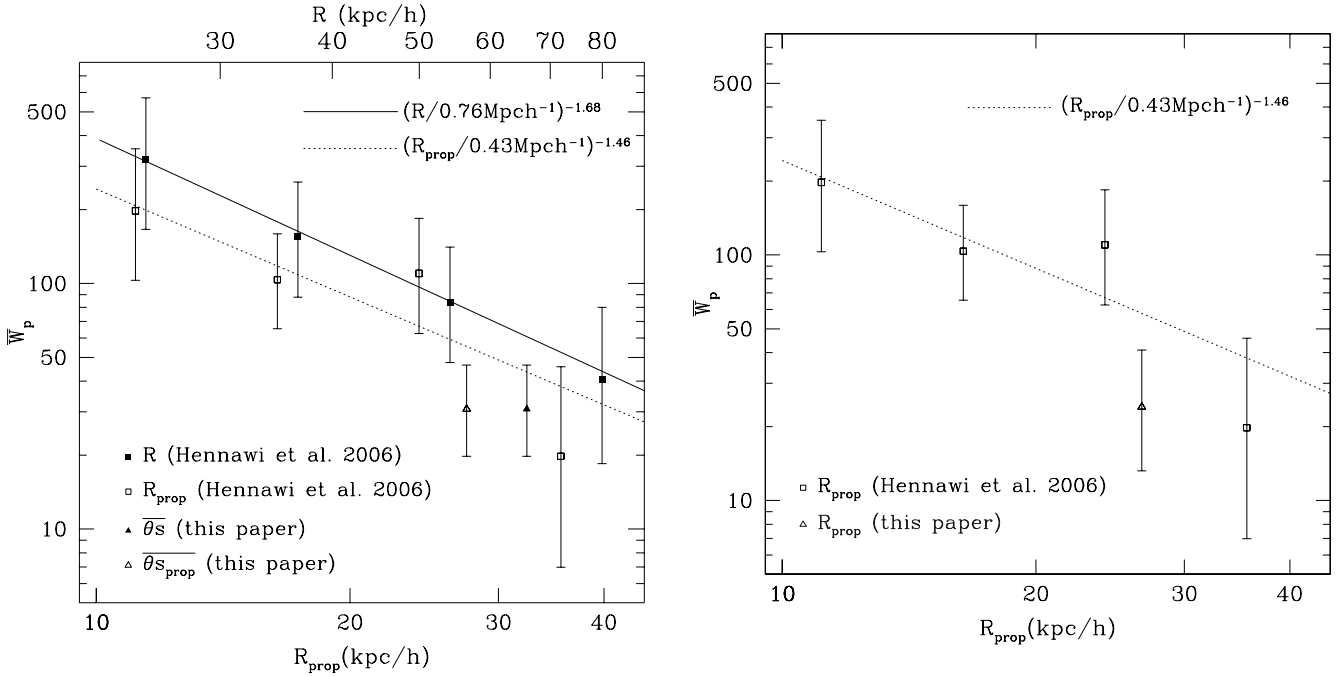

FIG. 4.—Projected correlation function, $\bar{W}_p$, of quasars on small scales. *Left*: The results of H06 in proper (*lower axis*) and comoving (*upper axis*) coordinates are compared to our mean DR4 KDE spectroscopic results averaged over $3.9'' < \Delta\theta < 5.2''$ and projected to a mean transverse separation at $z = 1.4$ (the mean redshift of both the DR4 KDE quasar sample and the subset of 16 quasars listed in Table 7), in proper (*open triangle*) and comoving (*filled triangle*) coordinates. The dotted (solid) line shows a power-law fit to the H06 data on proper (comoving) scales of $<100\,h^{-1}$ kpc ($<200\,h^{-1}$ kpc). *Right*: A similar comparison, but our data are now averaged over scales of 23.7 h^{-1} kpc $< R_{\rm prop} <$ 29.9 h^{-1} kpc and redshifts of $1.0 < z < 2.1$. The DR4 KDE binary quasar sample is spectroscopically complete for $A_g < 0.17$, $g < 20.85$, and $3.9'' < \Delta\theta < 5.2''$, and for 23.7 h^{-1} kpc $< R_{\rm prop} <$ 29.9 h^{-1} kpc over $1.0 < z < 2.1$. [*See the electronic edition of the Journal for a color version of this figure.*]

and find a best fit with $\bar{z} = 1.4$, $\sigma = 0.6$, $\beta = 0.65$, and $n = 3$ (see also Myers et al. 2007a). We have repeated our analyses using a spline fit instead, and our results differ by $\lesssim$2%.

To determine $\langle QR \rangle$ in a given bin, we use a random catalog with 1000 times as many points as the ($A_g < 0.17$, $g < 20.85$) KDE DR4 photometric quasar catalog. We total all QR counts in the *angular* bin of interest and normalize the result (divide by 1000). We then create a random catalog with points distributed according to equation (5) and determine the fraction of pairs that would lie within $|\Delta v_\parallel| < 2000$ km s^{-1} by Monte Carlo sampling to 0.1% precision. Multiplying this fraction by the normalized QR counts yields $\langle QR \rangle$. In a bin of $3.9'' < \Delta\theta < 5.2''$ we expect 30.3 QR counts. Over our full $N(z)$ distribution, we expect 0.0166 pairs with $|\Delta v_\parallel| < 2000$ km s^{-1}. Thus, $\langle QR \rangle = 0.503$, compared to $QQ = 16$ for the eight (nonunique) pairs in Table 7. The implied projected correlation function averaged over $3.9'' < \Delta\theta < 5.2''$ is thus $\bar{W}_p = 30.8^{+15.7}_{-11.0}$. We note that, for all candidate pairs, $QQ(3.9'' < \theta < 5.2'') = 40$, yielding an angular correlation of $\omega(\theta) = (40/30.3) - 1 = 0.320^{+0.366}_{-0.292}$, which is consistent with M07b.

Our sample in Table 7 is complete on angular scales of $3.9'' < \theta < 5.2''$. At the mean redshift of our sample ($\bar{z} = 1.40$), this angular range is equivalent to proper (comoving) scales of 23.5 h^{-1} kpc $< R_{\rm prop} <$ 31.4 h^{-1} kpc (56.5 h^{-1} kpc $< R <$ 75.3 h^{-1} kpc). We are not, however, strictly complete on these proper scales because of the evolution of $R_{\rm prop}(\theta)$. Our chosen cosmology, however, has little evolution in $R_{\rm prop}(\theta)$ over $1.0 < z < 2.1$, which means that we are spatially complete for proper scales of 23.7 h^{-1} kpc $< R_{\rm prop} <$ 29.9 h^{-1} kpc over $1.0 < z < 2.1$ (strictly $1.03 < z < 2.10$ in our chosen cosmology). We therefore consider two different measurements of $\bar{W}_p$, one that is angularly complete and one that is spatially complete but comprises fewer binaries. In the left panel of Figure 4, we plot $\bar{W}_p$ for the entire angularly complete sample in Table 7 (which we simply project back to the proper or comoving scales that correspond to $3.9'' < \theta < 5.2''$ at $z = 1.4$). In the right panel of Figure 4 we consider only those binaries in Table 7 that are in our spatially complete subsample (with 23.7 h^{-1} kpc $< R_{\rm prop} <$ 29.9 h^{-1} kpc and $1.0 < z < 2.1$). Note that it is straightforward to restrict our calculation of $\langle QR \rangle$ in equation (4) to $1.0 < z < 2.1$, as we can estimate the relative fraction of DR4 KDE quasars in this redshift range from equation (5).

Figure 4 demonstrates that our results using a complete, statistical sample of UVX binary quasars are broadly consistent with H06. To compare with the results of H06, we fit power laws, displayed in Figure 4, out to proper (comoving) scales of $<100\,h^{-1}$ kpc ($<200\,h^{-1}$ kpc) and integrate them over our scales of interest. For our angularly complete sample in Table 7, we find a value of $\bar{W}_p = 30.8^{+15.7}_{-11.0}$ for our data. The proper (comoving) power-law fit to the data from H06 implies a value of $\bar{W}_p = 55.1$ (60.4) over the same scales, which is a 1.5 σ (1.9 σ) difference. For the five binaries in our spatially complete clustering subsample, which covers scales of 23.7 h^{-1} kpc $< R_{\rm prop} <$ 29.9 h^{-1} kpc, we find a value of $\bar{W}_p = 24.0^{+16.9}_{-10.8}$, and the H06 data imply a value of $\bar{W}_p = 57.2$, which is 2.4 times (and 2.0 σ) higher than our result. We note that as we compare to a fit across the H06 data, the error budget from H06 is too small to impact our comparisons. A direct comparison to a single measurement and error from H06 is difficult, given the change in $\bar{W}_p$ with scale, but would certainly lead to a $<$2.0 σ detection.

5. DISCUSSION

We find that the projected correlation function of quasars at proper scales of $\sim$25 h^{-1} kpc has an amplitude that is a factor of 2.4 times lower than that determined by H06. H06 argue that clustering on these scales is $\sim$10 times higher than expected from projecting the quasar autocorrelation of Porciani et al. (2004) to smaller scales. Our data thus imply excess quasar clustering at

$\sim 25\,h^{-1}$ kpc of a factor of ~ 4, which is consistent with the quoted upper limit in M07b. Given that our sample is targeted differently than any previous samples of binary quasars have been (i.e., UVX, but otherwise regardless of the color similarity of the candidate components), and given our simple selection function, our work might be viewed as independently corroborating the evidence for excess quasar clustering on small scales that was first detected by Djorgovski (1991) and was confirmed with a larger sample by H06. We note that our binary quasar clustering subsample is largely independent of the sample used by H06, as of the eight binaries listed in Table 7, only two appear in Table 5.

The fact that we find far smaller excess clustering at $\sim 25\,h^{-1}$ kpc than do H06 is probably indicative of the complicated selection function and uncertain incompleteness of the sample used in H06. As the binaries in Table 7 are all at $z < 2$, but H06 include several $R_{\rm prop} \sim 25\ h^{-1}$ kpc binaries with $z > 2$, an interesting alternative possibility is that $\bar{W}_p$ is a function of both scale *and* redshift. Certainly, on large scales ($\gtrsim 1\ h^{-1}$ Mpc), quasars cluster twice as strongly at $z > 2$ as at $z < 1$ (e.g., Croom et al. 2005; Shen et al. 2007). The mean redshift of the H06 sample is $\bar{z} = 1.87$ (J. Hennawi 2007, private communication), compared to $\bar{z} = 1.42$ for our sample in Table 7. Croom et al. (2005) estimate the quasar bias on large (i.e., $\gtrsim 1\ h^{-1}$ Mpc) scales to follow the relation $b(z) = 0.53 + 0.289(1+z)^2$. Given that quasar clustering scales as b^2, the implied relative amplitude between quasar clustering in H06 and our sample is ~ 1.72. Scaling our measurement of $\bar{W}_p = 30.8^{+15.7}_{-11.0}$ by this factor implies that $\bar{W}_p = 53.0^{+27.0}_{-18.9}$, which is easily consistent with the value of $\bar{W}_p = 57.2$ implied by our fit to the H06 data in Figure 4. Scaling the $\bar{W}_p = 24.0^{+16.9}_{-10.8}$ estimate for our complete subsample ($\bar{z} = 1.60$) in the same way implies that $\bar{W}_p = 33.1^{+23.4}_{-14.9}$, which is lower than $\bar{W}_p = 57.2$ but consistent to $\sim 1\ \sigma$. Thus, multiplying our quasar clustering amplitudes on *small* scales by the implied bias evolution from quasar clustering on *large* scales somewhat reconciles our clustering amplitudes with the higher redshift results from H06. Consistent evolution of quasar clustering on large and small scales is a natural feature of merger-driven models of quasar origin (e.g., Fig. 17 of Hopkins et al. 2008).

Our analyses could be easily extended, as the 98 ($3'' \leq \Delta\theta < 6''$) DR4 KDE binary quasar candidates should contain ~ 40 binary quasars. If we split these 40 binary quasars into four redshift bins containing 10 binaries each, equation (5) suggests that the lowest redshift bin will be centered near $z = 0.8$ and the highest redshift bin near $z = 2.1$. If we assume that the Croom et al. (2005) estimate of quasar bias evolution [$b(z) = 0.53 + 0.289(1+z)^2$ at $\gtrsim 1\ h^{-1}$ Mpc] holds at $R_{\rm prop} \sim 25\ h^{-1}$ kpc, the relative amplitude of $\bar{W}_p$ in these bins will be ~ 5.1. By adopting Poisson errors, we find that having 10 objects in each redshift bin will distinguish a factor of 5.1 in amplitude at a significance of $2.2\ \sigma$, meaning that the DR4 KDE binary quasar candidate sample should contain sufficient data to determine whether quasar clustering evolution is similar on large and small scales. Alternatively, Shen et al. (2007) suggest a survey of quasar pairs at $z > 3$, where stronger quasar clustering may lead to a more significant detection of evolution. The DR6 KDE quasar catalog (G. T. Richards et al. 2008, in preparation), which will be selected to $i < 21$ ($g \lesssim 21.25$), should contain ~ 500 binary quasar candidates across a large redshift range ($0.4 \lesssim z \lesssim 5$) with which to pursue these goals in a single homogeneous sample.

6. CONCLUSIONS

We have presented a spectroscopic survey of binary quasar candidates with separations in the range $3'' \leq \Delta\theta < 6''$. Our candidates (see Table 1 of M07b) are a subsample of quasars photometrically classified in SDSS DR4 using the KDE technique of Richards et al. (2004). We define a binary as a quasar pair with a line-of-sight velocity difference of $\left|\Delta v_{\parallel}\right| < 2000$ km s^{-1} (see H06). We present 27 new sets of observations and identify both members of 22 candidate binary quasars. Of the 22 new pairs, 10 turn out to be binary quasars (of which ~ 2 might actually be lenses). This roughly doubles the number of known binary quasars with $3'' \leq \Delta\theta < 6''$ at $z \lesssim 2$ and $g < 21$. A further nine of our observed candidates are projected quasar pairs, and three contain a NELG or a star. This confirms that the KDE technique is $\sim 95\%$ efficient at selecting quasars (e.g., Richards et al. 2004; Myers et al. 2006, 2007a). When we combine this with observations from the literature (mainly from H06), we find that 46% of the DR4 KDE binary quasar candidates have now been observed, of which $\sim 47\%$ are binaries or lenses, $\sim 40\%$ are projected quasar pairs, and the remainder contain a nonquasar.

As our candidate binaries, beyond a UVX cut, are selected regardless of the *relative* colors of the quasars in the pair, we can try to assess the color similarity criteria that optimally select binary quasars. For quasars preselected with an already efficient approach such as the KDE technique, we find that a χ^2 color similarity statistic of $\chi^2_{\rm color} < 70$ will return 97% of binaries, lenses, and projected pairs (multiplied by the 95% completeness of the KDE technique itself) at 93% efficiency. Most of this efficiency in selecting quasar pairs comes from the KDE technique itself, as imposing no color similarity criterion is 87% efficient. We find that a color similarity cut of $\chi^2_{\rm color} < 20$, such as that used in H06, will miss around a third of all binary quasars. We stress that H06 expanded their sample to also include binary quasars with $\chi^2_{\rm color} \geq 20$ that contained a previously identified quasar. To select binary quasars while rejecting projected quasar pairs, we suggest a cut in the overlap of the photometric redshifts of the two candidate quasars in a pair. An overlap of $\gtrsim 0.03$ in the primary solution for the photometric redshift probability density functions of the pair can be constructed to be $\sim 95\%$ complete and $\sim 70\%$ efficient for binary quasars. Similarly, of course, the reverse probability cut of $\lesssim 0.03$, perhaps coupled with a $\chi^2_{\rm color} < 70$ cut to remove stars, can be used to reject binary quasars in favor of projected quasar pairs.

We measure the clustering of a complete sample of DR4 binaries on proper scales of $23.7\ h^{-1}$ kpc $< R_{\rm prop} < 29.9\ h^{-1}$ kpc. We find that, at $\sim 25\,h^{-1}$ kpc, quasars cluster with an amplitude that is 2.4 times, or $2.0\ \sigma$, lower than that determined by H06. As the mean redshift of the H06 sample is $\bar{z} = 1.87$, compared to $\bar{z} = 1.40$ for our sample, this can be interpreted as evidence of evolution in quasar clustering on scales of $\sim 25\,h^{-1}$ kpc. The implied evolution is broadly consistent with merger-driven models, where the quasar population is expected to evolve with consistent large- to small-scale clustering (e.g., Hopkins et al. 2008). We find no significant evidence for quasar clustering evolution at $\sim 25\ h^{-1}$ kpc in our sample alone. Assuming evolution in the binary quasar population at the level suggested for larger scales in Croom et al. (2005), we argue that observing all 98 pairs in the DR4 KDE candidate binary sample should be sufficient to detect any clustering evolution at proper scales of $\sim 25\ h^{-1}$ kpc for $z \lesssim 2.5$.

We thank the NOAO staff for their indispensible help and knowledge. In particular, we thank Buell Januzzi, without whose support this work would not have been possible in a timely fashion. A. D. M. and R. J. B. acknowledge support from NASA through grant NN6066H156, from Microsoft Research, and from the University of Illinois. G. T. R. acknowledges support from an Alfred P. Sloan Research Fellowship. D. P. S. acknowledges NSF support through grant AST-0607634. P. B. H. is supported by

NSERC. The authors made extensive use of the storage and computing facilities at the National Center for Supercomputing Applications and thank the technical staff for their assistance in enabling this work. We thank Robert Nichol and Alex Gray for their invaluable work on the KDE catalog.

Funding for the SDSS and SDSS-II has been provided by the Alfred P. Sloan Foundation, the Participating Institutions, the National Science Foundation, the US Department of Energy, the National Aeronautics and Space Administration, the Japanese Monbukagakusho, the Max Planck Society, and the Higher Education Funding Council for England. The SDSS Web site is http://www.sdss.org/.

The SDSS is managed by the Astrophysical Research Consortium for the Participating Institutions. The Participating Institutions are the American Museum of Natural History, Astrophysical Institute Potsdam, the University of Basel, Cambridge University, Case Western Reserve University, the University of Chicago, Drexel University, Fermilab, the Institute for Advanced Study, the Japan Participation Group, Johns Hopkins University, the Joint Institute for Nuclear Astrophysics, the Kavli Institute for Particle Astrophysics and Cosmology, the Korean Scientist Group, the Chinese Academy of Sciences (LAMOST), Los Alamos National Laboratory, the Max Planck Institute for Astronomy (MPIA), the Max Planck Institute for Astrophysics (MPA), New Mexico State University, Ohio State University, the University of Pittsburgh, the University of Portsmouth, Princeton University, the United States Naval Observatory, and the University of Washington.

REFERENCES

Adelman-McCarthy, J. K., et al. 2006, ApJS, 162, 38
Antonucci, R. 1993, ARA&A, 31, 473
Bahcall, J. N., Bahcall, N. A., & Schneider, D. P. 1986, Nature, 323, 515
Bahcall, J. N., Kirhakos, S., Saxe, D. H., & Schneider, D. P. 1997, ApJ, 479, 642
Barnes, J. E., & Hernquist, L. 1996, ApJ, 471, 115
Cao, L., Wei, J.-Y., & Hu, J.-Y. 1999, A&AS, 135, 243
Croom, S. M., & Shanks, T. 1996, MNRAS, 281, 893
Croom, S. M., et al. 2005, MNRAS, 356, 415
Djorgovski, S. 1991, in ASP Conf. Ser. 21, The Space Distribution of Quasars, ed. D. Crampton (San Francisco: ASP), 349
Djorgovski, S., & Spinrad, H. 1984, ApJ, 282, L1
Djorgovski, S. G., Courbin, F., Meylan, G., Sluse, D., Thompson, D., Mahabal, A., & Glikman, E. 2007, ApJ, 662, L1
Elvis, M. 2000, ApJ, 545, 63
Fukugita, M., Ichikawa, T., Gunn, J. E., Doi, M., Shimasaku, K., & Schneider, D. P. 1996, AJ, 111, 1748
Gehrels, N. 1986, ApJ, 303, 336
Hennawi, J. F., & Prochaska, J. X. 2007, ApJ, 655, 735
Hennawi, J. F., et al. 2006, AJ, 131, 1 (H06)
Hewett, P. C., Foltz, C. B., Chaffee, F. H., Francis, P. J., Weymann, R. J., Morris, S. L., Anderson, S. F., & MacAlpine, G. M. 1991, AJ, 101, 1121
Hewett, P. C., Foltz, C. B., Harding, M. E., & Lewis, G. F. 1998, AJ, 115, 383
Hopkins, P. F., & Hernquist, L. 2006, ApJS, 166, 1
Hopkins, P. F., Hernquist, L., Cox, T. J., Di Matteo, T., Robertson, B., & Springel, V. 2006, ApJS, 163, 1
Hopkins, P. F., Hernquist, L., Cox, T. J., & Kereš, D. 2008, ApJS, 175, 356
Hopkins, P. F., Lidz, A., Hernquist, L., Coil, A. L., Myers, A. D., Cox, T. J., & Spergel, D. N. 2007, ApJ, 662, 110
Inada, N., et al. 2003, Nature, 426, 810
———. 2008, AJ, 135, 496
Kochanek, C. S., Falco, E. E., & Muñoz, J. A. 1999, ApJ, 510, 590
Landy, S. D., & Szalay, A. S. 1993, ApJ, 412, 64
Lupton, R., Gunn, J. E., & Szalay, A. S. 1999, AJ, 118, 1406
Mason, K. O., et al. 2000, MNRAS, 311, 456
Mortlock, D. J., Webster, R. L., & Francis, P. J. 1999, MNRAS, 309, 836
Myers, A. D., Brunner, R. J., Nichol, R. C., Richards, G. T., Schneider, D. P., & Bahcall, N. A. 2007a, ApJ, 658, 85
Myers, A. D., Brunner, R. J., Richards, G. T., Nichol, R. C., Schneider, D. P., & Bahcall, N. A. 2007b, ApJ, 658, 99 (M07b)
Myers, A. D., et al. 2006, ApJ, 638, 622
Oguri, M. 2006, MNRAS, 367, 1241
Oguri, M., et al. 2005, ApJ, 622, 106
———. 2006, AJ, 132, 999
Peng, C. Y., et al. 1999, ApJ, 524, 572
Phinney, E. S., & Blandford, R. D. 1986, Nature, 321, 569
Pogson, N. R. 1856, MNRAS, 17, 12
Porciani, C., Magliocchetti, M., & Norberg, P. 2004, MNRAS, 355, 1010
Richards, G. T., et al. 2001, AJ, 121, 2308
———. 2004, ApJS, 155, 257
Rusin, D. 2002, ApJ, 572, 705
Schlegel, D. J., Finkbeiner, D. P., & Davis, M. 1998, ApJ, 500, 525
Schneider, D. P., et al. 2003, AJ, 126, 2579
———. 2007, AJ, 134, 102
Shanks, T., Bean, A. J., Ellis, R. S., Fong, R., Efstathiou, G., & Peterson, B. A. 1983, ApJ, 274, 529
Shen, Y., et al. 2007, AJ, 133, 2222
Spergel, D. N., et al. 2007, ApJS, 170, 377
Sramek, R. A., & Weedman, D. W. 1978, ApJ, 221, 468
Stoughton, C., et al. 2002, AJ, 123, 485
Vanden Berk, D. E., et al. 2001, AJ, 122, 549
Veron-Cetty, M.-P., et al. 2004, A&A, 414, 487
Weinstein, M. A., et al. 2004, ApJS, 155, 243
York, D. G., et al. 2000, AJ, 120, 1579